Ab initio study of scintillating lanthanide oxyhalide host materials

Materials Research Express

RECEIVED
5 July 2015

REVISED
14 August 2015

ACCEPTED FOR PUBLICATION
27 August 2015

PUBLISHED
5 October 2015

PAPER

Ab initio study of scintillating lanthanide oxyhalide host materials

G Shwetha[1], **V Kanchana**[1], **N Yedukondalu**[2] **and G Vaitheeswaran**[2]

[1] Department of Physics, Indian Institute of Technology Hyderabad, Ordnance Factory Estate, Yeddumailaram, Hyderabad-502 205, Telangana, India

[2] Advanced Centre of Research in High Energy Materials (ACRHEM), University of Hyderabad, Prof C R Rao Road, Gachibowli, Hyderabad-500 046, Telangana, India

E-mail: kanchana@iith.ac.in

Keywords: density functional theory, electronic structure, optical properties, scintillators, luminescence

Abstract

We have investigated the structural, electronic, and optical properties of layered oxyhalides using plane wave pseudopotential and full-potential linearized augmented plane wave methods based on density functional theory. The structural properties calculated using local density approximation (LDA) are in reasonable agreement with the experiments compared to generalized gradient approximation (GGA) for these layered materials. We find these compounds to be wide band gap insulators with band gap ranging from 3.6 to 7.8 eV. The band gap decreases on moving from Cl to I, while it increases from the La to Lu series. The calculated refractive index show LaOCl and LaOBr to be optically isotropic in the lower energy regions in-spite of its anisotropic structure. From the present calculations, we predict bromides and iodides to be better scintillating host materials to exhibit Ce-activation among the studied compounds and especially lanthanum-based compounds are found to be more promising among the studied ones.

1. Introduction

Investigation of new inorganic scintillators with a high light yield, short decay time, good energy resolution, and stopping power has been an intense area of research during the past few decades due to their applications in high-energy physics, medical imaging, radiation detection and homeland security. The activated rare-Earth oxyhalides REOX (RE = Y, La, Gd; X = F, Cl, Br) have been widely studied due to their applications as x-ray intensifying phosphors [1–3]. Lanthanum oxyhalides LaOX (X = Cl, Br, I) have unique and excellent electrical, magnetic, optical, and luminescent properties [4]. The study of the luminescence properties of LaOX (X = F, Cl, Br):Eu phosphors has been carried out by Park *et al* [5] and they observed that the emission spectra shifts to lower wavelengths as the size of the anion decreases. Eagleman [6] and his co-workers determined the scintillating properties and decay time of REOX (RE = Y, La, Gd and Lu; X = Cl, Br, I):Ce, and they found that GdOBr:0.5%Ce has the highest light output among the investigated compounds. Oxyhalides of lanthanum and terbium activated with cerium are found to be potential oxygen-dominated phosphors. In the conversion of x-rays to visible light, these phosphors are considered to be superior because of their conversion efficiency, and are popularly known as *x-ray image converters*, [7] and they also find applications in x-ray image intensifier tubes, fluoroscopic screens, radiographic intensifier screens, lamps, and cathode ray tubes. Among the family of lanthanum-based scintillators, cerium-doped lanthanum trihalides, $LaCl_3$ [8], $LaBr_3$ [9–12], $LaBr_{3-x}I_x$ [13], LaF_3 [14], and LaI_3 at high temperature below 100 K [15] are known as bright scintillators and have received lot of attention during the past because of their fast decay time, excellent scintillation output, and energy resolution. When compared with oxyhalides, trihalides are known to be hygroscopic in nature, which makes them difficult to be handled [6]. The hygroscopic nature of rare-Earth oxyhalides decreases with increasing ionic size of rare-Earth atom (i.e., the smaller the rare earth, the, greater the hygroscopic nature of the material). Density is also a parameter used to measure scintillation. The higher the density, the larger the absorption and stopping power [16]. These oxyhalides are high-density materials. LuOI is found to have the highest density among all the studied compounds. Moreover, lanthanum-based crystals are preferred over other compounds because of their

high detection efficiency and less radioactive (compared to lutetium) nature. The rich chemistry of lanthanum has paved the way for numerous lanthanum-based compounds. Moreover, the cations La^{3+} and Ce^{3+} have similar bonding patterns and, covalent and ionic radii [17], enabling La-based compounds to be more effective for Ce-activation. Theoretical studies on the Ce-doped Y, La oxyhalide compounds [18] predicted that the luminescence increases from F to I. Here we are interested in studying the electronic structure and optical properties of the host compound, because there are very few theoretical studies available with LDA functions, and also find a better candidate for Ce activation. (Throughout this paper, *X* stands for Cl, Br, I in case of the La series and Br, and I in the case of the Lu series).

2. Computational details

We have performed first-principles calculations by employing a plane wave pseudopotential (PW/PP) approach based on density functional theory (DFT) [19, 20] as implemented in Cambridge Serial Total Energy Package (CASTEP) [21–23]. We have used Vanderbilt-type ultrasoft pseudopotentials [24] for electron-ion interactions to perform the geometry optimization, and norm-conserving pseudopotentials are used for calculating dynamical properties. The exchange-correlation potential of Ceperley and Alder [25] parametrized by Perdew and Zunger [26] in the LDA and GGA with the Perdew–Burke–Ernzerhof (PBE) [27] parametrization are used for the electron–electron interaction, and crystal is relaxed with Broyden–Flecter–Goldgarb–Shanno minimization scheme [28]. For each of these compounds, the following plane wave basis orbitals were used: La: $5s^2, 5p^6, 5d^1, 6s^2$; Lu: $4f^{14}, 5p^6, 5d^1, 6s^2$; O : $2s^2, 2p^4$; Cl : $3s^2, 3p^5$; Br : $4s^2, 4p^5$; and I : $5s^2, 5p^5$. We tested the total energy dependence on plane wave cut-off energy and k-mesh according to the Monkhorst–Pack scheme [29]. It is found that the cut-off energy for LnOX (Ln = La, Lu; X = Cl, Br, I) is 420 eV, and k-mesh of $8 \times 8 \times 4$ is appropriate because the change in total energy is minimal. In the geometry relaxation, the self-consistent convergence threshold on total energy is 5×10^{-7} eV/atom.

In addition, we have also used the full potential linearized augmented plane wave method explicitly to study the electronic structure and optical properties which is incorporated through the WIEN2k software package. This is one of the most accurate methods for calculating the physical and chemical properties of materials. In this method, a unit cell of the crystal is partitioned into the atomic sphere region and the interstitial region. Within the atomic sphere, the wave function is expanded as atomic like function, and in the interstitial region, a plane wave basis is used. The core electrons are treated fully relativistically and valence electrons are treated semi-relativistically. Throughout our calculations, we have set the $R_{MT} \times K_{max}$ value at 9, where R_{MT} is the smallest of the muffin-tin radii, K_{max} is the plane wave cut-off energy for the expansion of wave function in the interstitial region, and the charge density was Fourier-expanded up to $G_{max} = 12$. Tetrahedron method is used for the k-point integration over the Brillouin zone [30]. We have used PBE-GGA [27] and Tran–Blaha modified Becke–Johnson potential (TB-mBJ) [31–34] functionals for calculating the band gap values we found improved band gap with TB-mBJ functional over standard PBE-GGA. In addition we also used TB-mBJ functionals with new parameter for *A*, as suggested by Jishi *et al* [35], and we found improved band gap when compared to the TB-mBJ functional with the default parameters. The internal atomic positions were relaxed by using PBE-GGA for the exchange-correlation functional at the experimental lattice constants. For the electronic structure calculations, we have used $13 \times 13 \times 5$ k-mesh, as it is well-known that the optical properties require denser k-mesh, and we increased the same to $22 \times 22 \times 10$.

3. Results and discussion

3.1. Structure, electronic properties and chemical bonding

Lanthanide oxyhalides, LnOX (Ln = La, Lu; X = Cl, Br, I), crystallize in the primitive tetragonal structure (space group P4/nmm, 129) with two molecular formula units or six atoms per unit cell. The two metal ions (Ln^{+3}) are positioned at (0, 0.5, *v*) and the two chalcogen and halogen anions (O^{-2}, X^{-1}) are located at (0, 0, 0) and (0, 0.5, *u*), respectively, where *v* and *u* are internal parameters of La and X atoms, respectively. Hygroscopic nature is inversely related to the ionic size (Y < La < Lu), which follows the order Y > La > Lu. For all theoretical calculations, it is necessary to obtain the equilibrium structure. Therefore, we optimized both lattice geometry and ionic positions to get a fully relaxed crystal structure of these systems. The equilibrium structural parameters, such as lattice constants and volume, are obtained using the PW/PP method within both LDA and GGA and are summarized in table 1 along with the experimental data [36–38]. The obtained ground state properties using LDA functional are in reasonable agreement with the experimental data over GGA results for these layered materials. Hence, we are convinced that the LDA functional is good enough to reproduce the experimental trends in spite of their layered structure. We also noticed that lattice constants (*a*, *c*) and volume (*V*) increase from La → Lu (Cl → I) and this is due to the cation–anion size difference between La^{+3}, Lu^{+3}

Table 1. Caculated lattice constants (a, c in Å), volume (V, in $Å^3$), and density (gm/cm^3) of LnOX (Ln = La, and Lu, and X = Cl, Br, I) compounds compared with the experimental results [36–38].

Compound	Method	a	c	V	density
LaOCl	LDA	4.09	6.78	113.94	5.55
	GGA-PBE	4.20	6.98	123.25	5.13
	Expt.	4.119	6.883	116.78	5.41
LaOBr	LDA	4.15	7.17	123.54	6.31
	GGA-PBE	4.20	7.76	137.37	5.67
	Expt.	4.159	7.392	127.86	6.09
LaOI	LDA	4.14	8.85	151.45	6.18
	GGA-PBE	4.21	10.00	178.23	5.32
	Expt.	4.144	9.126	156.71	5.97
LuOBr	LDA	3.78	7.92	113.26	7.94
	GGA-PBE	3.86	9.68	144.11	6.24
	Expt.	3.7646	8.3540	118.39	7.59
LuOI	LDA	3.86	8.96	133.33	7.91
	GGA-PBE	3.94	9.77	152.49	6.92
	Expt.	3.8585	9.189	136.81	7.72

(Cl^-, Br^- and I^-). As mentioned in the previous section, density is one of the important criteria for good scintillation; the higher the density, the greater the stopping power and the absorption of radiation. These oxyhalide compounds have higher density than the corresponding trihalides ($LaCl_3$-3.84, $LaBr_3$-5.06, LaI_3-5.63 gm cm^{-3}). Calculated density values with different functionals are given in table 1, and from this table, we can clearly see that density values increase on from the La to the Lu series among the studied compounds—suggesting that LuOX is denser.

Electronic structure calculations are quite important to understand the optoelectronic process. We have calculated the electronic band structure by using the TB-mBJ functional and the corresponding figures are shown in figure 1. These are wide band gap insulators with LaOCl, LuOI possessing indirect band gap and LaOBr, LaOI, LuOBr possessing direct band gap. The TB-mBJ functional is relatively less-expensive compared to GW calculations and can reproduce the band gaps comparable to the experiment. Interestingly, we found the band gap values to decrease down the column from Cl to I in all the Ln series, which is in good agreement with the recent experimental results [39]. In addition, the band gap increases from La →Lu compounds and the corresponding band gap values of LnOX compounds are given in table 2. We have also calculated band gap values using the TB-mBJ functional with new parameters for *A* as suggested by Jishi *et al* [35], and we found improved band gap when compared to TB-mBJ functional with default parameters and are given in table 2 (TB-mBJ-New). We found the width of the valence band to increase from Cl to I in the Ln series, and also from La →Lu. The calculated density of states (DOS) for the investigated compounds using TB-mBJ functional is shown in figure 2 for the LnOX series. X-p (X = Cl, Br and I), O-p states are present in valence band of the LaOX series, where these states are around 0 to −2.9 eV for LaOCl. Moving down the periodic table from Cl to I, these widths increase to −3.0, −3.4 eV for LaOBr, LaOI compounds. Additionally Lu-*f* states are present in valence band in the case of the LuOX series, which is absent in LaOX, and as with the LaOX series, the width of the valence band increases from −3.8 to −4.1 eV proceeding from LuOBr to LuOI. The conduction band is of La-*f*, *d* states for the LaOX series, and in the case of the LuOX series, these states are formed by Lu-*d*, X-*d* states; from Br to I, these states shift to lower energy regions in LnOX series, thereby decreasing the band gap of the compounds. The DOS certainly might be influenced by the inclusion of U (LDA+U calculations). It is possible that the empty states would be shifted up, and the occupied states shifted down. In our calculations, we have not included U, because Chaudhry *et al* [18] have already reported that for these series of compounds, with the inclusion of U, the position of f-level will change the band gap only by the order of a tenth of an eV, . Since the exclusion of U would not notably change the results, we made our calculations without taking U into account. In addition, it should be noted that the TB-mBJ functional is sufficient and works well for the rare-Earth systems as mentioned by David *et al* [31].

In order to predict the trend of luminescence, we compared the electronic structure of LnOX (Ln = La, Lu, X = Cl, Br and I) with that of YOX (X = F, Cl, Br and I) from our previous calculations [42]. In case of YOX, band gap decreases from F to I, and the width of the valence band increases from F to I. When we compare the YOX series with that of LaOX and LuOX, we observe the band gap values decrease from Y to La then increases in the LuOX series. The width of the valence band decreases from Y to La and increases in the Lu series. In YOX compounds, valence band arises mainly from O-*p*, X-*p* (X = F, Cl, Br, and I) states and conduction band minimum is mainly due to Y-*d*, X-*d* states. The width of the valence band follows the order

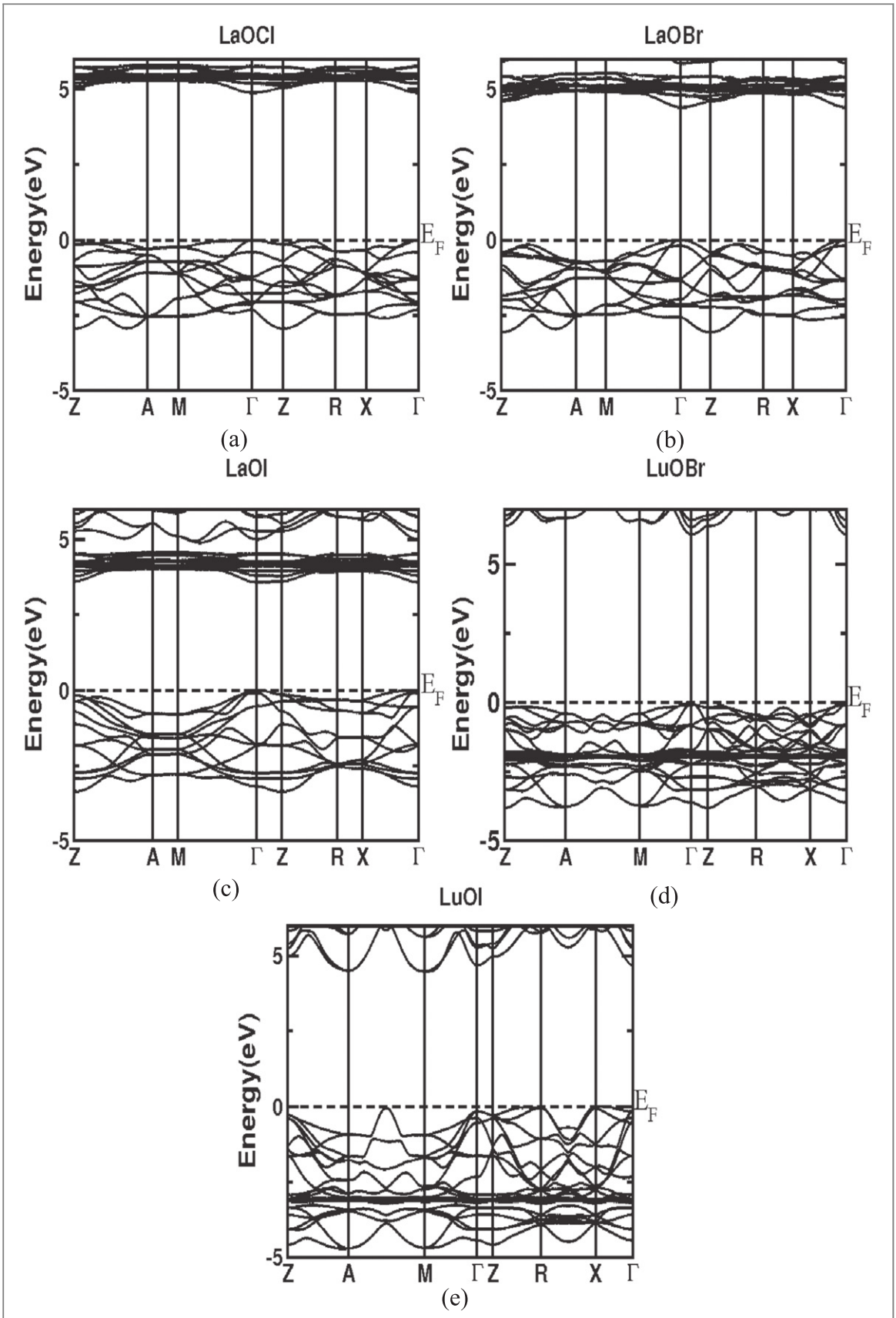

Figure 1. Calculated band structures of LaOCl, LaOBr, LaOI, LuOBr, and LuOI using the TB-mBJ functional.

Table 2. Calculated band gap of LnOX (Ln = La, Lu; X = Cl, Br, and I) compounds (in eV) using GGA and TB-mBJ, TB-mBJ with specific parameters indicated with TB-mBJ-New along with available band gap values.

	LaOCl	LaOBr	LaOI	LuOBr	LuOI
GGA	4.07	3.68	3.26	4.17	3.28
TB-mBJ	4.88	4.31	3.58	6.09	4.49
TB-mBJ-New	5.76	5.30	4.54	7.80	6.31
Others [18]	4.3	4.0	3.0	—	—
exp [39–41]	5.53,5.23	5.35,4.8	4.82	—	—

LuOI > YOI > LuOBr > YOBr > YOCl > LaOI > LaOBr > LaOCl > YOF. Reduction in the band gap from Cl to I might result in more number of electron hole pairs, which might be a good indication for the luminescence to increase from Cl to I.

Chemical bonding of the compounds can be very well-explained by using the Mulliken population analysis. We calculated Mulliken bond population [43] in order to analyse the type of bonding in a LaOI compound. The Mulliken charges of O, I, and La are found to be −0.76, −0.07, 0.83 $|e|$, respectively, and from these values, it is clear that O and I are more electronegative towards La, demonstrating the ionic nature of these compounds. The bond population value of La–O bond is 0.43, which is less then 0.5, indicating the ionic nature of the bond [43]. We also calculated the percentage of ionicity based on the population ionicity [44], using the following formula:

$$P_i = 1 - \exp\left(- \frac{P_c - P}{P} \right) \quad (1)$$

The calculated population ionicity values for La—O is 0.73, which is greater than 0.5, indicating the strong ionic nature of these compounds.

3.2. Optical properties

Optical properties aid us to understand the scintillation mechanism and the type of transition involved. We increased the k-mesh to 22 × 22 × 10 in order to ensure proper convergence. From the imaginary part of dielectric function all the other optical parameters are calculated by using the Kramers–Kronig relations. Our main focus is on the absorption spectra of these compounds and is a function of photon energy (figure 3). Based on these spectra, we predict the scintillation in these host compounds.

The absorption spectra of LaOCl and LaOBr are similar; they differ from LaOI because of its additional states. Consequently, the difference between the first and second valence bandwidths decreases from LaOCl to LaOI, which results in one broad peak in LaOI, whereas it is two for LaOCl, LaOBr. The absorption spectra shows an increase in width from Cl to I. In our case, the width of the absorption spectra follows the trend as follows: LaOCl < LaOBr < LaOI < LuOBr < LuOI. The lower edge of absorption spectra is shifted to lower-energy regions because of decrease in the band gap. The imaginary part of dielectric function suggests values for the absorption spectra, and the calculated real and imaginary part of dielectric function is shown in figure 4. The calculated refractive index is shown in figure 5, and from this figure, we can clearly see that LaOCl and LaOBr are optically isotropic in the low-energy regions, which is an essential requirement for ceramic scintillators. The refractive index values for all the compounds increases, reaches a maximum value (these maximum values are given in table 3 along with the static refractive index values) and then decreases. As shown in table 3, it is clear that the difference between n_{xx} and n_{zz} values increases as we move from Cl to I, indicating that anisotropy increases from Cl to I. The calculated refractive index values show the opposite trend as that of the band gap. The lower-energy spectral region of absorption spectra in the case of LaOX compounds is due to transition of electrons from X-*p*, O-*p* states to La-*d* states. As to the LuOX series, these transitions are from X-*p*, O-*p*, Lu-*f* states to Lu-*d*, X-*d* states.

There are numerous scintillators available with Ce-activation, and in order to study the Ce-activation in the presently studied compounds, we compared the three criteria given by Canning *et al* [18, 45–47]. The three criteria are (i) the size of the band gap, (ii) the energy difference between the valence band maximum (VBM) of the host and Ce 4f level, and (iii) the level of localization of *d*-character of the excited state. The criterion (i) and (ii) are based on band gap values, whereas criteria (iii) is about localization of the conduction band state. With the decrease in the band gap, the number of carriers available for luminescence increases. Furthermore, the difference between the VBM and Ce-*f* level decrease (as a result, there is a probability of transferring electrons from host to Ce-site) resulting in an increase in the luminescence. In the presently studied compounds, band gap decreases from Cl to I and increases from La to Lu, indicating an increase in the luminescence from Cl to I and a

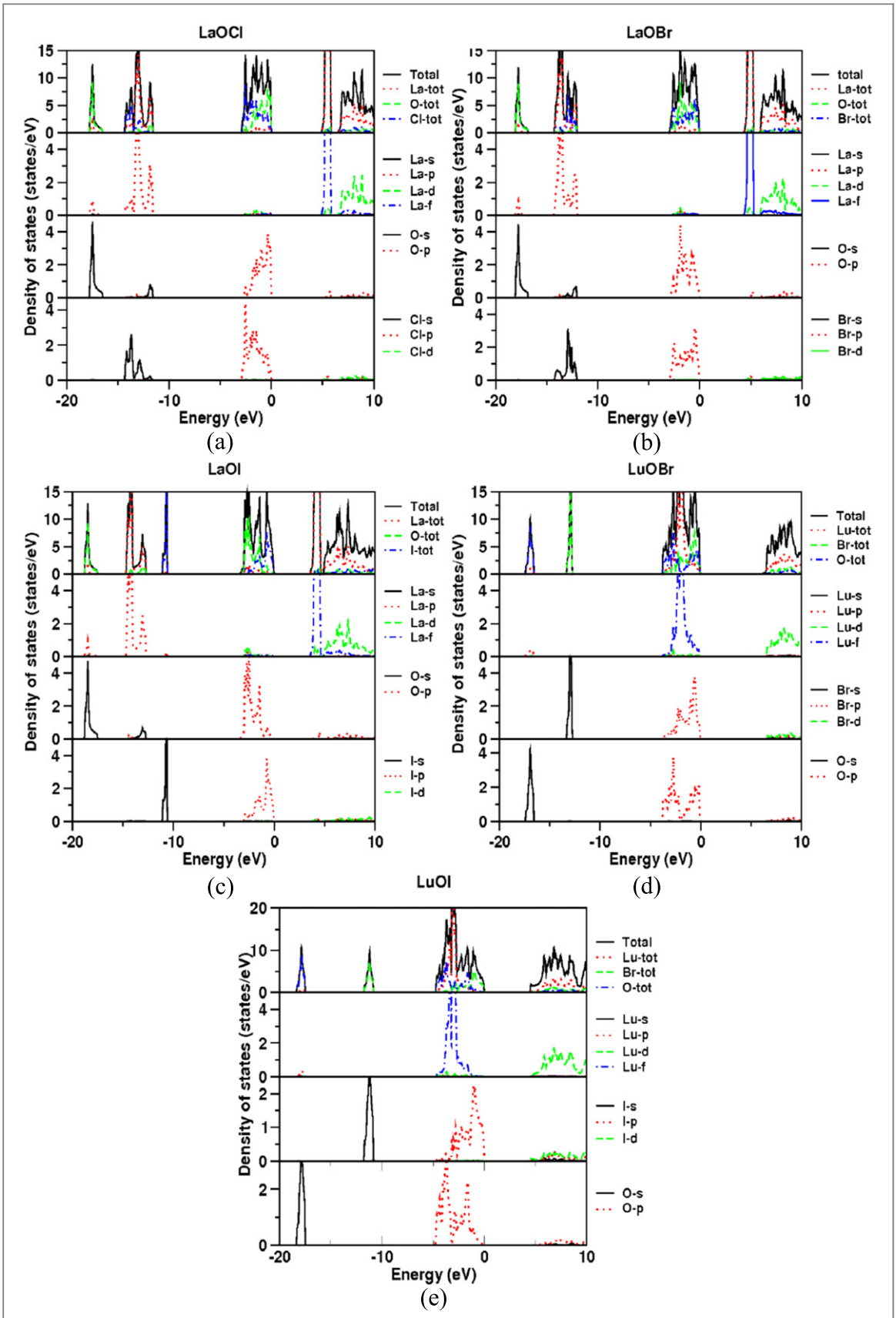

Figure 2. DOS of LnOX (Ln = La, Lu, and X = Cl, Br, I) compounds using the TB–mBJ functional.

probable decrease from La to Lu. To support our results, we also calculated the maximum light output [48, 49] or scintillation yield, which is approximated by considering the transfer efficiency and quantum efficiency to be unity, which is given by

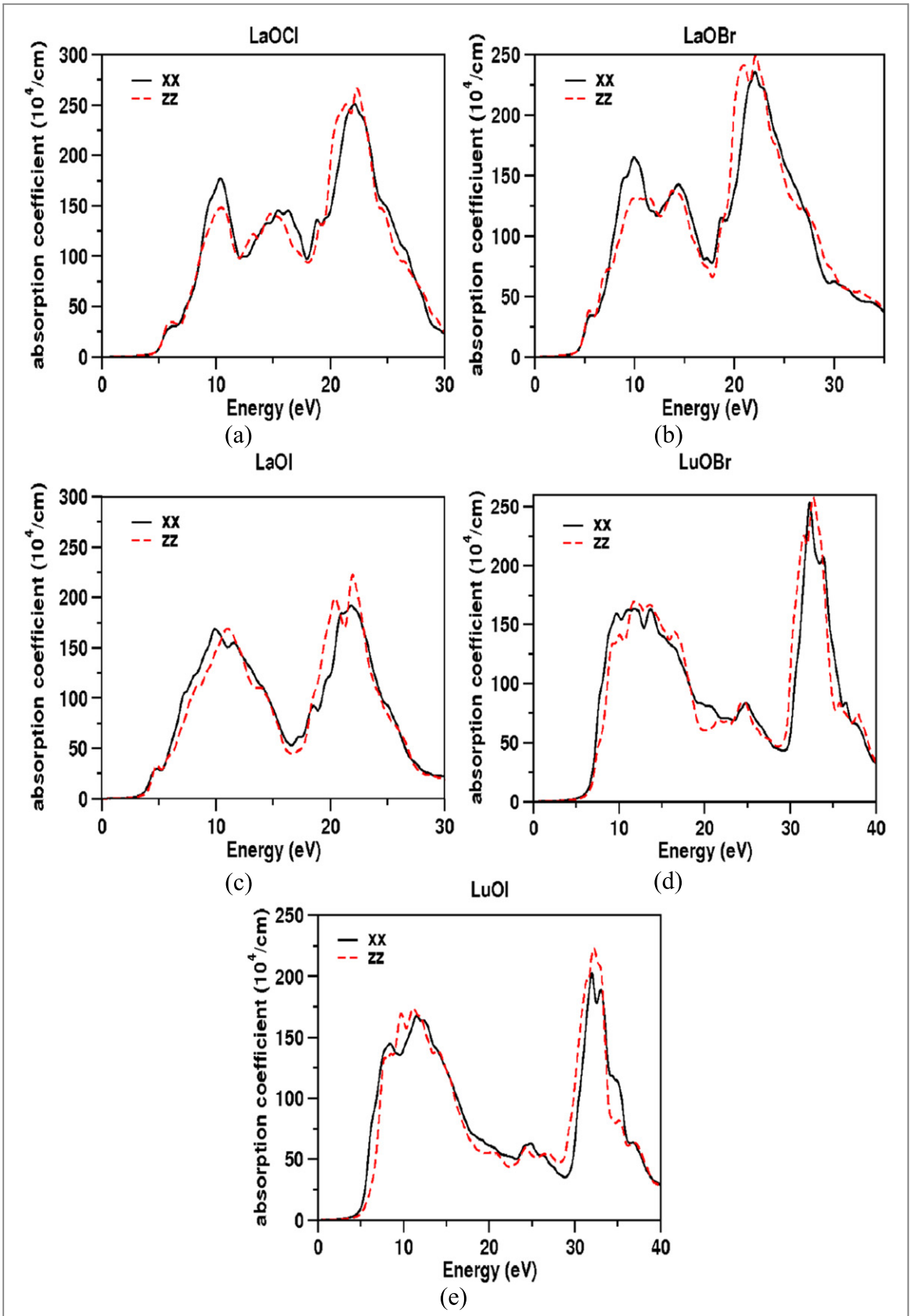

Figure 3. Calculated absorption coefficient of LnOX (Ln = La, Lu, and X = Cl, Br, I) compounds.

$$L_{Max} = \left(\frac{0.5}{E_g}\right)10^6\left(\frac{photons}{Mev}\right) \quad (2)$$

where E_g is the band gap (in eV) of the compounds. The absolute light yield [50] calculation involves longitudinal optical phonon frequencies and static dielectric function. Here, we are interested in maximum approximate

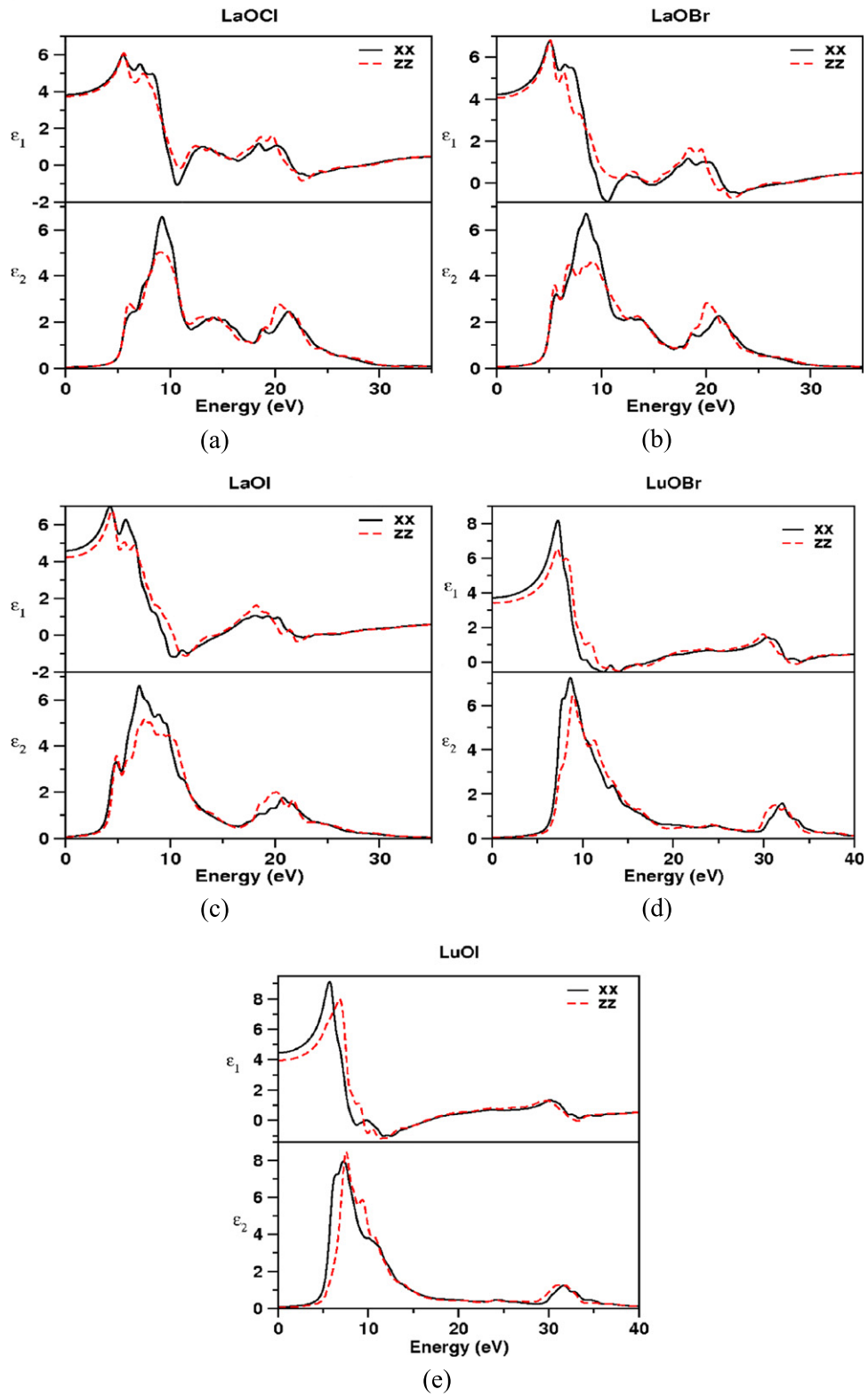

Figure 4. Dielectric function of LnOX (Ln = La, Lu, and X = Cl, Br, I) compounds using the WIEN2k software package.

light yield from Cl to I rather than the absolute value in order to predict the trend of luminescence from Cl to I. These values might be even more than the absolute values. These light yield values are expected to be greater for ionic compounds. The studied compounds are found to be ionic, which is confirmed by the chemical bonding. We have calculated the maximum scintillation yield of these compounds from the TB-mBJ band gap values with modified parameters (TB-mBJ with default parameters) and these values are 6.0584×10^4(7.3529×10^4), 6.6525×10^4(8.0645×10^4), 7.1922×10^4(9.0909×10^4), and 8.4602×10^4(1.1111×10^5) photons/Mev for YOX (X = F, Cl, Br, and I) compounds respectively. These values for LnOX are found to be

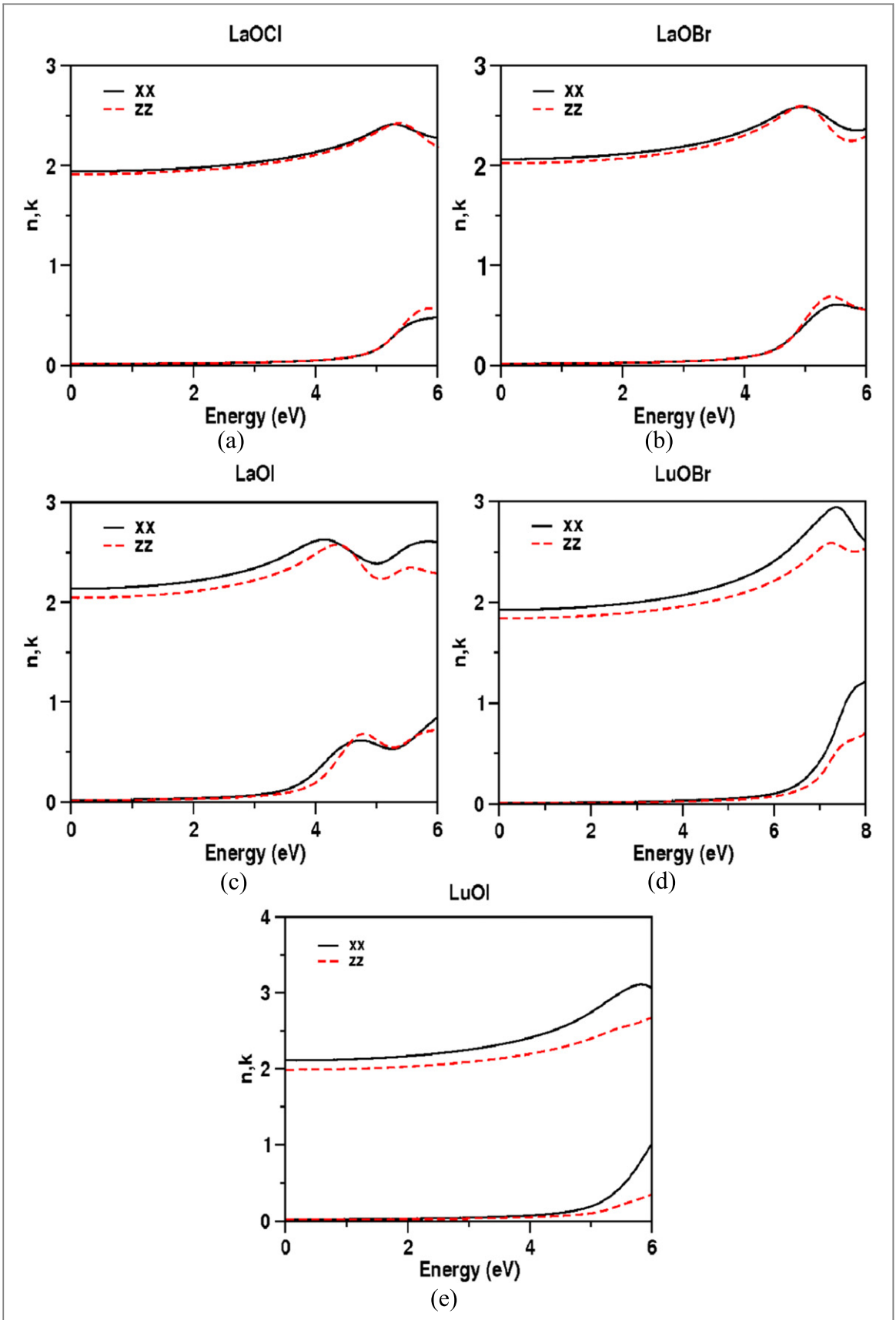

Figure 5. Calculated refractive index of LnOX (Ln = La, Lu, and X = Cl, Br, I) compounds using the TBmBJ functional.

$8.6760 \times 10^4(1.0246 \times 10^5)$, $9.4340 \times 10^4(1.1598 \times 10^5)$, $1.0996 \times 10^5(1.3963 \times 10^5)$, $6.3776 \times 10^4(8.02061 \times 10^4)$, $7.9189 \times 10^4(1.1126 \times 10^5)$ photons/Mev for LaOCl, LaOBr, LaOI, LuOBr, and LuOI respectively, which are quite larger than the absolute values. We have compared the light yield of LuI_3 used

Table 3. Static refractive index values, maximum value of refractive index for LnOX (Ln = La, Lu; X = Cl, Br, and I) compounds.

	LaOCl	LaOBr	LaOI	LuOBr	LuOI
$n(0)_{xx}$	1.94	2.06	2.13	1.92	2.11
$n(0)_{zz}$	1.91	2.02	2.04	1.84	1.98
$n(\omega)_{xx}^{max}$	2.41	2.59	2.62	2.94	3.10
$n(\omega)_{zz}^{max}$	2.42	2.59	2.57	2.59	2.95

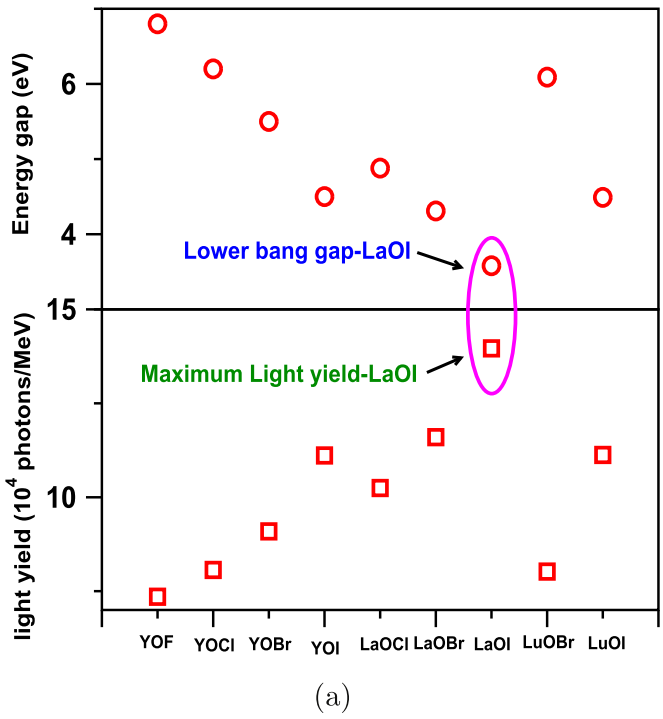

Figure 6. Energy gap and Maximum light yield values of LnOX (Ln = Y, La, Lu, and X = Cl, Br, I) compounds using the TB-mBJ functional.

by van Leof *et al* [51]. They reported the light yield to be in the range of 98000–100000, which is quite high compared to the corresponding oxyhalides. This supports the data indicating that the light yield of oxyhalides are less than that of their corresponding halides. $LaBr_3$[9, 52] and $LaCl_3$[8] are reported to have light yield around 61000, 46000 photons/MeV. These results are not identical to ours, because ours present the approximate light yield, and it is possible to determine the trend of luminescence in the relevant compounds using this approximation. Bessiere [15] has also reported that LaI_3 does not show any Ce-activation at room temperature but does at high temperatures. The present studied compounds have lesser light yields compared to their corresponding halides, but the calculated electronic structural and optical properties may improve the light yield of these compounds further. The maximum light yield values and the energy band gap of these compounds are shown in figure 6. There, it is evident that the light yield increases both from Cl to I (with decrease in the band gap) and from Y to La, then decreases in Lu. Among all the compounds, LaOI has the highest light yield, which makes it the best scintillator of those reviewed. The maximum light yield values increase from Cl to I, which supports the hypothesis that the luminescence increases from Cl to I, and that lanthanum-based compounds, particularly LaOI are good scintillators compared with the others discussed herein. The trend of valence band width, absorption spectra, band gap, and the maximum light yield of these compounds are shown in table 4. From the table 4, we can see that both the absorption spectra and, light yield increase from F to I, which results in increased luminescence from F to I. The light yield values increase from Y to La, then, in the case of Lu, decrease. From this, we can conclude that the La-based compounds have the potential to be good scintillators. By considering the electronic structure, optical properties, and maximum light yield, we can expect that the luminescence will increase from Cl to I and that La-based compounds are good scintillators as compared with Y and Lu, especially with regard to LaOI. Our prediction is in good agreement with the data reported by Eagleman *et al* [6], who reported that all oxybromides and oxyiodides show better Ce-activated characteristics, which is in agreement with our prediction that luminescence increases from F to I. They also reported that YOBr:1% Ce^{3+},

Table 4. The trends of width of valence band(VB), absorption spectra (AS), band gap, and maximum light yield from F to I, Y to Lu in LnOX (Ln = Y, La, Lu; X = F, Cl, Br, and I) compounds, where ↑ denotes an increasing trend, ↓ represents a decreasing trend.

	F to I	Y to La	La to Lu
Width of the VB	↑	↓	↑
Width of the AS	↑	↓	↑
Band gap	↓	↓	↑
Maximum light yield	↑	↑	↓

LaOI: 2% Ce^{3+}, and GdOCl:0.5% Ce^{3+} are three combinations of attractive pairs with high density and moderate light yields. This is also in agreement with our results, where we predict LaOI to be a better scintillating host compound. Experimental studies with Ce-doping in REOX by Eagleman *et al* [6] report YOBr, LuOBr to be better than iodides with greater luminescence. On the other hand, Chaudary *et al* [18] speculated that the reduced luminescence in YOI: Ce (LuOI:Ce) might be due to some defects and suggested that LaOI might be a better candidate.

4. Conclusions

Ab initio calculations are carried out in order to study the electronic, optical properties of rare-Earth oxyhalides —which are less hygroscopic when compared to rare-Earth halides. All the studied compounds are insulators with LaOCl and LuOI possessing indirect band gap, while LaOBr, LaOI, LuOBr are direct band gap insulators. From the calculated refractive index, it is found that LaOCl, LaOBr are isotropic in the low-energy region though they are structurally anisotropic, which is a requirement for the ceramic scintillators. From the calculated electronic structure, we expect the luminescence to increase from Cl to I, and bromides and iodides are found to be good scintillators, and LaOI is expected to be the best among the studied compounds.

Acknowledgments

V K would like to acknowledge IIT Hyderabad for the HPC facility. G S would like to acknowledge MHRD for the fellowship, IIT Hyderabad for the computational facility. N Y and G V thank Center for Modelling Simulation and Design-University of Hyderabad (CMSD-UoH) for providing computational facility.

References

[1] Blasse G and Bril A 1967 *J. Chem. Phys.* **47** 5139
[2] Rabatin J G 1982 *J. Electrochem. Soc.* **129** 1552
[3] Starick D, Golovkova S I, Gurvic A M and Herzog G 1988 *J. lumin.* **40** 199
[4] Rambabu U, Mathur A and Buddhudu S 1999 *Mater. Chem. Phys.* **61** 156
[5] Park J K, Lim M A, Kim C H, Park H D, Han C H and Choi S Y 2003 *J. Mat. Sci. Lett.* **22** 477
[6] Eagleman Y D, Bourret-Courchesne E and Derenzo S E 2011 *J. Lumin.* **131** 669
[7] Rabatin J G 1974 *X-ray image converters utilizing lanthanum and gadolinium oxy halide luminous materials activated with thulium* U. S. Pat. 3795814.
[8] vanLoef E V D, Dorenbos P, van Eijk C W E, Krämer K and Güdel H U 2001 *IEEE Trans. Nucl. Sci.* **48** 341
[9] vanLoef E V D, Dorenbos P, van Eijk C W E, Krämer K W and Güdel H U 2002 *Nucl. Instr. Meth. Phys. Res.* A **486** 254
[10] Menge P R, Gautier G, Iltis A, Rozsa C and Solovyev V 2007 *Nucl. Instr. Meth. Phys. Res.* A **579** 6
[11] de Haas J T M and Dorenbos P 2008 *IEEE. Trans. Nucl. Sci.* **55** 1086
[12] Salacka J S and Bacrania M K 2010 *IEEE. Trans. Nucl. Sci.* **57** 901
[13] Birowosuto M D, Dorenbos P, Krämer K W and Güdel H U 2008 *J. Appl. Phys.* **103** 103517
[14] Moses W W and Derenzo S E 1990 *Nucl. Instr. Meth. Phys. Res.* A **299** 51
[15] Bessiere A, Dorenbos P, van Eijk C W E, Krämer K W, Güdel H U, de Mello Donega C and Meijerink A 2005 *Nucl. Instr. Meth. Phys. Res.* A **537** 22
[16] Lecoq P, Annenkov A, Gektin A, Korzhik M and Pedrini C 2006 *Inorganic Scintillators for Detector Systems Physical Principles and Crystal Engineering* (Heidelberg: Springer-Verlag)
[17] Porter-Chapman Y D, Bourret-Courchesne E, Taylor S E, Weber M J and Derenzo S E 2006 *IEEE Trans. Nucl. Sci. Symp. Conf. Record* **3** 1578
[18] Chaudhry A, Canning A, Boutchko R, Porter-Chapman Y D, Bourret-Courchesne E, Derenzo S E and Jensen N G 2009 *IEEE T. Nucl. Sci.* **56** 949
[19] Hohenberg P and Kohn W 1964 *Phys. Rev.* **136** B864
[20] Kohn W and Sham L J 1965 *Phys. Rev.* **140** A1133
[21] Payne M C, Teter M P, Allan D C, Arias T A and Joannopoulos J D 1992 *Rev. Modern Phys.* **64** 1045
[22] Segall M D, Lindan P J D, Probert M J, Pickard C J, Hasnip P J, Clark S J and Payne M C 2002 *J. Phys.: Condens. Matter* **14** 2717

[23] Milman V, Winkler B, White J A, Pickard C J, Payne M C, Akhmatskaya E V and Nobes R H 2000 *Int. J. Quantum Chem.* **77** 895
[24] Vanderbilt D 1990 *Phys. Rev.* B **41** 7892
[25] Ceperley D M and Alder B J 1980 *Phys. Rev. Lett.* **45** 566
[26] Perdew J P and Zunger A 1981 *Phys. Rev.* B **23** 5048
[27] Perdew J P, Burke K and Ernzerhof M 1996 *Phys. Rev. Lett.* **77** 3865
[28] Fischer T H and Almlof J 1992 *J. Phys. Chem.* **96** 9768
[29] Monkhorst H J and Pack J D 1976 *Phys. Rev.* B **13** 5188
[30] Blöchl P E, Jepsen O and Andersen O K 1994 *Phys. Rev.* B **49** 16223
[31] Singh D J 2010 *Phys. Rev.* B **82** 205102
[32] Koller D, Tran F and Blaha P 2011 *Phys. Rev.* B **83** 195134
[33] Koller D, Tran F and Blaha P 2012 *Phys. Rev.* B **85** 155109
[34] Tran F and Blaha P 2009 *Phys. Rev. Lett.* **102** 226401
[35] Jishi R A, Oliver B T and Sharif A A 2014 *J. Phys. Chem.* C **118** 28344
[36] Flahaut J 1974 *J. Solid State Chem.* **9** 124
[37] Zimmermann S, Pantenurg I and Meyer G 2007 *Acta Cryst.* E **63** i156
[38] Zimmermann S and Meyer G 2007 *Acta Cryst.* E **63** i193
[39] Kim D, Park S, Kim S, Kang S G and Park J C 2014 *Inorganic Chem.* **53** 11966
[40] Choubey A, Som S, Biswas M and Sharma S K 2011 *J. Rare Earth* **29** 345
[41] Starick D, Lange W and Herzog G 1988 *J. Therm. Anal.* **33** 889
[42] Shwetha G, Kanchana V and Valsakumar M C 2014 *J. Appl. Phys.* **116** 133510
[43] Mulliken R S 1955 *J. Chem. Phys.* **23** 1833
[44] Lingam B C H, Ramesh Babu K, Tewari S P and Vaitheeswaran G 2011 *J. Comput. Chem.* **32** 1734
[45] Canning A, Boutchko R, Chaudhry A and Derenzo S E 2009 *IEEE Trns. Nucle. Sci.* **56** 944
[46] Canning A, Chaudhry A, Boutchko R and Jensen N G 2011 *Phys. Rev.* B **83** 125115
[47] Boutchko R, Canning A, Chaudhry A, Borade R, Bourret-Courchesne E and Derenzo S E 2009 *IEEE Trns. on Nucle. sci.* **56** 977
[48] Rodnyi P A 1997 *Physical Process in Inorganic Scintillators* (Boca Raton, FL: CRC Press)
[49] Birowosuto M D and Dorenbos P 2009 *Phys. Status Solidi* A **206** 9
[50] Vali R 2007 *J. Lumin.* **127** 727
[51] Birowosuto M D, Dorenbos P, van Eijk C W E and Gudel H U 2006 *J. Appl. Phys.* **99** 123520
[52] van Loef E V D, Dorenbos P, van Eijk C W E, Krmer K and Gdel H U 2001 *Appl. Phys. Lett.* **79** 1573